

UC Berkeley

newReplication/Extension Papers 2019 - 2020

Title

Visual Field Maps of the Visual Cortex

Permalink

<https://escholarship.org/uc/item/6k5084pj>

Authors

Bharghavan, Priyanka
Raza, Aida
Shane, Olivia
et al.

Publication Date

2020-05-01

Supplemental Material

<https://escholarship.org/uc/item/6k5084pj#supplemental>

Visual Field Maps of the Visual Cortex

Priyanka Bharghavan, Aida Raza, Olivia Shane, Riya Shrestha

Cognitive Science and Psychology Undergraduate Laboratory @ Berkeley

Undergraduate Student Mentor: Kunal Kapoor

Graduate Student Mentor: Brooke Staveland

University of California, Berkeley

Abstract

fMRI imaging measures brain activity by detecting changes in the brain that are associated with blood flow and can be used in order to determine the size and location of visual field maps. This study measured BOLD responses in humans to understand spatial summation by showing them spatial contrast pattern images through vertical and horizontal apertures. Nonlinear responses can be computed from the visual field responses, from which the spatial summation ratio is calculated. A ratio of less than one indicates a smaller response to exposure to a full aperture or contrast image than predicted by the linear model. Datasets were analyzed using MATLAB, producing eccentricity maps of the visual cortices from stimuli. BOLD response curves identify the intensity of the maps within a particular voxel. The eccentricity maps can then be overlain on anatomical representations of the brain, characterizing the various visual field cortices. Methods of fMRI data analysis are confirmed with the results of this study.

Key Words: BOLD response, visual field cortex, V1-V3, CSS model, SOC model, MATLAB, eccentricity

Introduction

The human visual cortex is located in the occipital lobe of the brain. Within the visual cortex, it is possible to find visual field maps, which are cortical regions that record and respond to spatial information in the visual field (Wandell, Brewer, & Dougherty, 2005). fMRI is a valuable tool to visualize cortical maps and identify active cortical regions when presented with a visual stimulus. fMRI imaging measures brain activity by detecting changes in the brain that are associated with blood flow and can be used in order to determine the size and location of visual field maps. The BOLD signal stands for blood oxygen level dependent and measures the changes in blood flow across regions in the brain by detecting changes in the oxygenation levels as oxygen is transferred from the blood to the brain tissues (Aguirre et al., 1998). It is possible to locate and measure visual field maps in the cortex by observing which regions of the brain are active when presented with specific visual stimuli. (Wandell, Dumoulin, & Brewer, 2007)

The early visual cortex consists of visual field maps V1, V2, and V3. These are separate cortical regions that take on visual processing functions. It was previously thought that the early visual cortex was only involved in early stage rudimentary visual processing, but new evidence suggests it is also responsible for high level visual computation. The high resolution buffer hypothesis states the early visual areas are necessary for processing precise spatial information. This hypothesis is grounded in computational models of the visual system, which show that feature detection, object recognition, and spatial precision are visual tasks that are intertwined. Additionally, anatomical features of V1 provide clues about its function. The visual field in V1 is arranged in retinotopic coordinates that allow for the precise capture of visual data. Receptive fields typically thought to only perform high-order processing have large visual fields that

capture more spatial information but lose spatial resolution. V1 is thought to be involved in higher order processing because it preserves precise data that would otherwise be lost as spatial data is collected. The paper proposes that early visual cortex fields are “geometric computational engines,” collecting precise data and performing geometric computations that determine “contours, surfaces, and shapes” (Lee, 2003).

Some key methods of fMRI analysis are multivariate analysis, real-time analysis, and model-based analysis. For analysis, the brain regions are divided into three dimensional units called voxels. fMRI image processing analyses the response of these voxels. Multivariate analysis takes in information from voxels spanning large distances to understand spatial patterns. This method uses techniques from machine learning to divide voxels into classes. A classifier is used to find the weight of each voxel, and then look at patterns of voxel weights across populations of voxels. Based on activity patterns in the data, the model can measure cognitive tasks like facial recognition and memory. Real-time analysis uses data collected during the fMRI scan to adjust the experiment while it is happening in ‘real time.’ A common technique is fMRI neurofeedback. In this method, data is collected in real time, then shown to the patient to influence their brain activity in a particular region. Model-based analysis uses computational analysis to model high level cognitive processes such as decision-making. In this method, game theory and reinforcement learning show how social interactions and decision-making results respectively impact future interactions. This data can be correlated with brain activity to generate a model which predicts neural signaling in specific situations (Cohen et al., 2017).

To further develop hypotheses on function and relationships between visual cortices, a fundamental understanding of its methods are necessary prior to making any such conclusions

Methods

Stimuli

This experiment uses stimuli in the form of high contrast grayscale images. The stimuli were in three separate sets of sets 1, 2 and 3 and the subjects were given a central fixation task as the stimuli in each set were presented. The code has the stimuli presented both artificially and naturally, to capture the advantages of both. Sets 1 and 2 presented their images in the form of artificial noise patterns, while set 3 had distinct natural objects being shown to the subject, such as carrots and elephants.

For the first set, stimuli set 1, the images were high-contrast grayscale images constructed at a resolution of 600 x 600 pixels and occupied a field of view of 21-29 degrees of retinal angle. Stimulus set one consisted of 69 stimuli each with 30 frames; the use of multiple frames were to average out unwanted variability of any specific pattern. During the trial, 30 frames of the stimulus 1 set were presented over a duration of 3 seconds and the following stimuli were presented with a gap of at least 5 seconds..

For stimulus sets 2-3, the stimuli were band-pass filtered grayscale images constructed with a resolution of 256 x 256 pixel, which was necessary for the band-pass filter, due to the filter's matrix of dimension being 21 x 21. This is important because the cornea can only pick up on certain frequencies and band pass filters remove high frequency and low frequency tones. The dimensions of 21 x 21 are applied based on previous data on visual stimuli that indicated that this specific dimension allows for stimulation of a certain cortex of the brain that is being replicated in this experiment. The resolution was upscaled to 800 x 800 later, for presentation purposes, and occupied a field of view of 12.7 degrees of retinal angle. Stimulus set 2 consisted of 156

stimuli, each consisting of multiple frames (most typically 9) and were presented in a random order. For stimulus sets 2 and 3, 9 frames were presented sequentially over a span of 3 seconds. The following stimuli were separated temporally by at least 5 seconds. Stimuli set 3 is similar to stimulus set 2, however this set consisted of 35 distinct, recognizable object images instead. Only one frame was given to each stimulus so the subject saw the same image flash 9 times over the 3 second interval.

CSS Model

The compressive spatial summation (CSS) model predicts uses the following computation to predict responses to a stimuli with varying locations in the visual field: a stimulus is weighted and summed using an isotropic 2-dimensional Gaussian and then transformed by a static power-law nonlinearity. Fitting this model consists of three major sub-processes: *stimulus processing*, *model fitting*, and *resampling*. Once the data from a given dataset and relevant stimuli are loaded onto MATLAB, we must ensure each stimulus will be efficiently processed in subsequent computations. Consequently, we concatenate the stimuli along the third dimension, resize them to 100 x 100, and reshape them into a “flattened” format. This is solely to reduce the computational time. This concludes the stimulus processing portion of the CSS Model fitting.

Next, we utilized MATLAB’s `fitnonlinearmodel.m` function, which to resample, evaluate multiple initial seeds, and perform stepwise fitting. We defined an initial seed for the parameters of the CSS model— namely the row index (R), column index (C), and standard deviation (S) of the 2D Gaussian; the gain parameter (G); and the exponent of the power-law nonlinearity (N)— as well as the bounds of the parameters. Implementing the model requires defining a function that intakes a vector of parameters and a matrix of stimuli in order to output a predicted response

to the stimuli. We thus used an anonymous function that mirrors the overall structure of the model by calculating the dot product between the stimulus and the 2D Gaussian, raising it to the exponent of the power-law nonlinearity, and multiplying that value by the gain parameter. We then defined the final model specification by using a stepwise fitting scheme that optimizes all the model parameters in two fittings. In doing so, we avoided local minima and subsequently reached a more accurate solution. A version of the coefficient of determination will quantify the goodness of fit by computing variance in the data relative to 0, so we defined this metric and the index of the voxel to fit it. All the aforementioned data is then used to define an “options struct” that we passed through the `fitnonlinearmodel` function in order to inspect the results of the model. These results and their visual manifestations are discussed in the next section.

In order to run cross-validation and bootstrapping resampling schemes, we defined new options structs that specify leave-one-out cross-validation and 100 bootstraps, respectively, and pass them through the `fitnonlinearmodel` function. By now, the model has been fitted to the full dataset, so we use it to compute the response of the model to a point stimulus with varying locations in the visual field. The visualization for this predicted response are discussed in the next section.

SOC Model

The second-order contrast (SOC) model is an extension of the CSS model, but with the addition of computing the second-order contrast. With a broader scope than the CSS model, which only analyzes how the location and size of the stimulus reveal the response, the SOC model analyzes how an arbitrary grayscale image relates to the response of the stimuli. Computing the response of the SOC model requires performing stimulus pre-processing (part

one and two), preparing the model for fitting, and finally, getting the model fitting and results. Part one of the stimulus pre-processing takes the stimuli and puts it in the dimensions we need, in order to get the contrast image later on. In part two, we do the actual stimulus pre-processing, applying the Gabor filters, in order to pick up on the contrast in that voxel. Once the data from a given dataset and relevant stimuli are loaded onto MATLAB, we perform part one the stimulus pre-processing. The overall goal of this is to make the data more accessible for analysis at the end. First, we extracted the stimuli we need, only fitting the first 99 out of 156 stimuli, as it was calculated in previous fMRI studies that it is standard to take 99 to 100 stimuli frames to get the image. We then did pre-computations, which included resizing the stimulus to reduce the computational time. We made sure all the values are between 0 & 254, and rescaled to range [0,1] to ensure that the image fits on the screen. We then subtracted off the background noise, setting it equal to zero in order for the image to come out clearly and then assigned different pixel values to the different shades (pixel vals between -.5 and .5, background is 0). Finally, pad the stimulus with zeros to reduce edge effects. After inspecting one stimulus, the image will appear on the screen, as a grayscale image showing the stimulus response.

We then move onto part two of the stimulus pre-processing. The purpose of this section of code is to transform the grayscale image from part one into a contrast image. This will provide a visual representation of how each voxel is related to each other. To accomplish this, Gabor filters are applied to the grayscale image. These filters analyze the frequency of the image to highlight certain features. This filtering process is used often in visual processing and models the way the visual cortex integrates visual information. (Khaleefah et al., 2019) The application of the filter normalizes the data and encodes the data as sine waves in matrices. The gabor function

is a complex sinusoid multiplied by a 2D Gaussian. Then 2 new parameters, r and s , are introduced. The r parameter is an exponent parameter and the s parameter is a saturation parameter. These parameters are used to highlight the relationship between individual frames. These processes assign a new value to each pixel in the original grayscale image and create a contrast image.

Next, we prepared the model for fitting. We again utilized MATLAB's `fitnonlinearmodel.m` function. We defined input parameters, and then fitted some of the parameters as the rest were already fixed. The parameters are $[R \ C \ S \ G \ N \ C]$. As mentioned, R is the row index of the center of the 2D Gaussian, C is the column index of the center of the 2D Gaussian, S is the standard deviation of the 2D Gaussian, G is a gain parameter, N is the exponent of the power-law nonlinearity, and C is a parameter that controls the strength of second-order contrast. Helper functions are defined and combined in the final model. The `socfun` helper function computed a weighted average and summed the stimuli values. The `gaufun` helper function turns the parameter values into a 2D Gaussian. The final SOC model combines these helper functions.

The final model is implemented in the function, `modelfun`, in which the six parameter values and stimuli values are input and the model computes the predicted response based on the normalized data. We next defined seeds for model parameters. The seed is the initial value that is run through the model. In the SOC model, 16 initial seeds were chosen and input into the `fitnonlinearmodel` function to find the seed that yields the optimal parameter values. Once the parameter values are set, the `modelfun` function is well defined and the results can be plotted to visualize the BOLD response to visual stimuli.

Results

Stimuli

All images were presented as grayscale images. The stimuli were given at a specific 21-30 degree of retinal angle as mentioned to target a particular cortex. Images presented in Figure 1 indicate the presence of the band-pass filtering to obtain the necessary processing for the next two models.

CSS Model

The final parameter estimates generated by the fitted CSS model were used to map the neuronal population receptive field (pRF) location ± 2 pRF sizes. The pRF, depicted by the red circle in **Figure 2-1**, explains measured fMRI responses to the visual stimuli and thereby forms the basis for visual field maps. Regarding the measurements themselves, we generated a bar graph to represent BOLD responses to the series of visual stimuli.

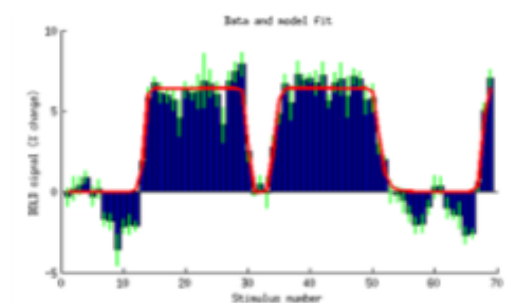


Figure 2-2: Visualizing the data and the CSSmodel fit based on the BOLD signal (%change)

SOC Model

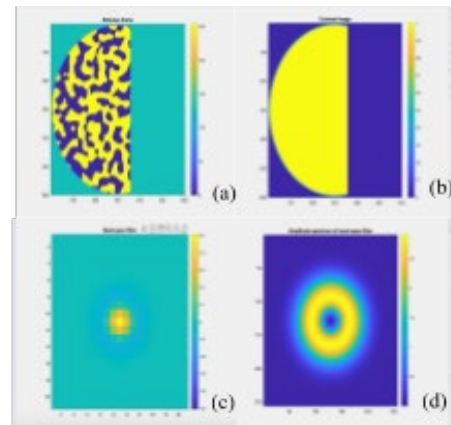


Figure 1: (a) the original stimulus frame (b) example of a contrast pattern presented at different location sin the visual field (c) the band pass filter is able to take a weighted contrast image, and summed using an isotropic 2-D Gaussian and then gets applied with a nonlinear transformation to get a response (d) an amplitude spectrum of the Fourier domain

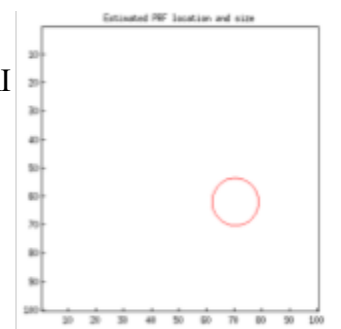


Figure 2-1: Estimated visualisation of the parameter estimates

Figure 2-2 depicts this data in blue, its associated error bars in green, and the model fitting in red. **Figure 2-3** represents a mapping of the CSS model's predicted response to some new stimuli, where lighter colors represent the presence of a strong visual response in a given area.

The result of part one image preprocessing is the grayscale image in **Figure 3-1**. This image is generated by simple rescaling functions and image processing techniques. The whole image is rescaled to 150 x 150 and the values of each pixel is rescaled to a number in the range [0,1].

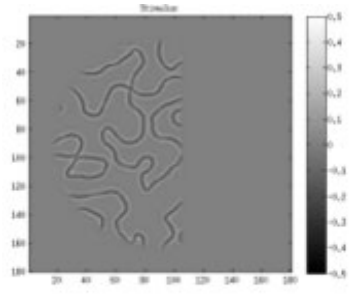


Figure 3-1: Extracting the stimuli to concatenate along the third dimension

Subtracting background noise assigns each pixel a value between $[-0.5, 0.5]$, as seen on the grayscale legend in

Figure 3-1.

The result of part two preprocessing is the contrast image in **Figure 3-2**. This image is generated by normalizing the stimulus values. The application of gabor filters and fitting model parameters normalizes the data. These processes assign new weight to the pixels based on the values of the frequency as determined by the gabor filters.

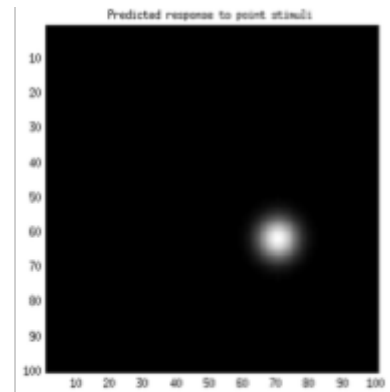


Figure 2-3: Predicted response of the mode to a point stimulus that is positioned at different locations in the visual field

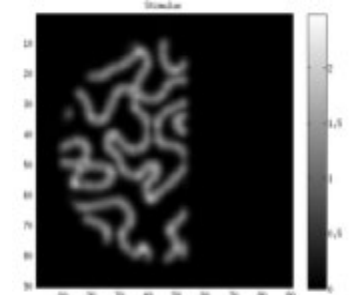


Figure 3-2: Inspecting one of the stimuli after performing stimulus pre-processing

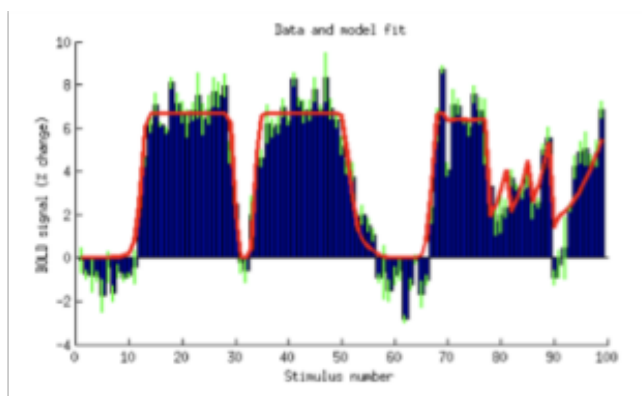


Figure 3-3: Visualizing the data and the SOC model fit to get the BOLD signal response curve.

The results of the model are shown in **Figure 3-3**. The BOLD function is defined by the average output of the SOC model function for each input: stimulus 1 to stimulus 99. The model takes in values of the $[R \ C \ S \ G \ N \ C]$ parameters and values of the stimulus and predicts the response to the

stimuli based on the normalized data. The normalized data is defined by a 2D Gaussian. The SOC model function is fit by the fitnonlinearfunction which assigns the optimal value to the parameters. Once the parameters are defined, the SOC model is plotted and results in the graph shown in **Figure 3-3**. Simulating the responses of the SOC model produces **Figure 3-4**, where certain values of the parameter are specified for the model. These parameters are matched to the typical values found in V3.

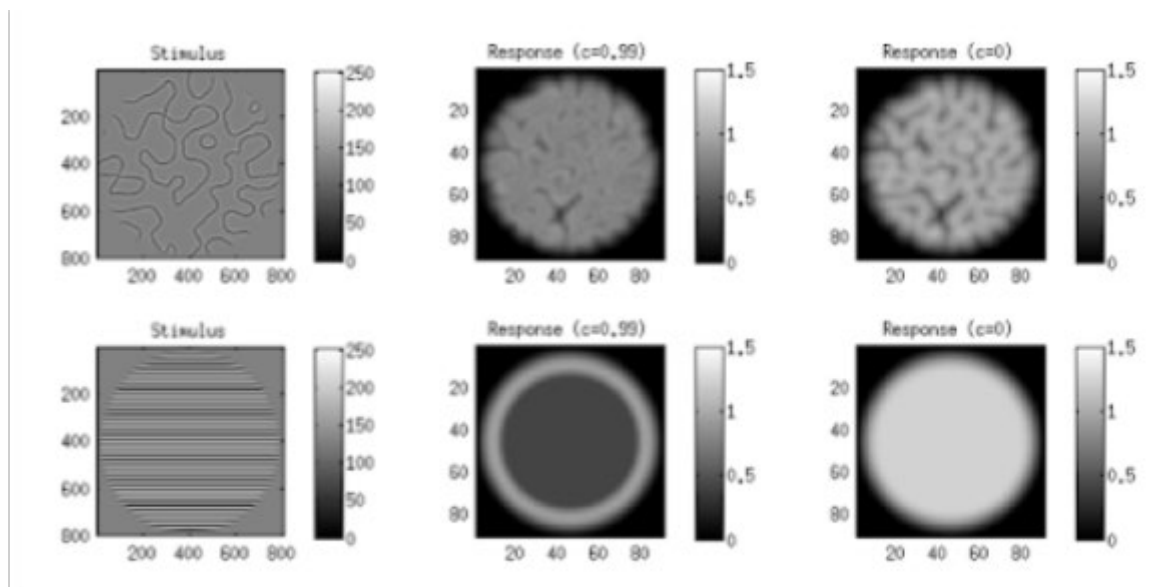


Figure 3-4: Visualizing the simulation results of the SOC model results

Analysis of Results

The CSS model has 100% contrast stimuli presented to the visual field. GLM and pRF fits were computed for data of each voxel. Nonlinear optimization of the responses then indicated a weighted sum of the curves to get the BOLD curve. Here, we showed how the code fits the CSS model to an example voxel from a provided dataset. **Figure 2-1** shows the estimated pRF location and size for the particular voxel. The BOLD data curve is visualized with **Figure**

2-2 with the data fit, from which the predicted response to point stimuli can be seen with **Figure 2-3**.

For the SOC model, stimuli with Gabor filters are presented to the visual field for local contrast. With the SOC model being more general, we can explain how an arbitrary grayscale image relates to the response from another dataset with **Figure 3-4**. The values for this dataset are matched to the typical values found in V3, and we get the computed response as seen in the figure.

Conclusion

The functional MRI has given the scientific community a greatly informative means of exploring human visual field maps. The combination of advances in MR technology and new analytical methods will continue to provide new information about the visual field maps. Many new computational methods, including diffusion-weighted imaging with tractography, MR-spectroscopy, and MR-relaxometry, will contribute to more clear and explicit information regarding the structures of the visual cortex. As technological growth progresses, questions involving the plasticity, development and function of the visual cortex will continue to be discovered.

Acknowledgements

This paper was supported by the Undergraduate Lab @ Berkeley. We thank our graduate student mentor, Brooke Staveland (UC Berkeley Neurosciences) for helping us understand the fundamentals of fMRI, fMRI analysis, and MatLab. We also extend our thanks to Dr. Mark D'Esposito (UC Berkeley Psychology) for providing the backing to make this paper possible.

References

1. Cohen, J., Daw, N., Engelhardt, B. et al. (2017). Computational approaches to fMRI analysis. *Nat Neurosci*, 20, 304–313.
2. Lee, T. S. (2003). Computations in the early visual cortex. *Journal of Physiology-Paris*, 97, 121–139.
3. Khaleefah, Shihab Hamad, et al. “The Ideal Effect of Gabor Filters and Uniform Local Binary Pattern Combinations on Deformed Scanned Paper Images.” *Journal of King Saud University - Computer and Information Sciences*, 2019,
4. Gabor Filters, www.cs.utah.edu/~arul/report/node13.html.
5. S A Engel, G H Glover, B A Wandell, Retinotopic organization in human visual cortex and the spatial precision of functional MRI., *Cerebral Cortex*, Volume 7, Issue 2, Mar 1997, Pages 181–192,
6. Lee, T. S. (2003). Computations in the early visual cortex. *Journal of Physiology-Paris*, 97(2–3), 121–139.
7. Balasubramanian, M., Polimeni, J., & Schwartz, E. L. (2002). The V1–V2–V3 complex: quasiconformal dipole maps in primate striate and extra-striate cortex. *Neural Networks*, 15(10), 1157–1163.
8. Jezzard P., Matthews P.M., Smith S.M. (2001). Functional MRI: an introduction to methods. “Oxford: Oxford University Press”

9. Aguirre, G., Zarahn, E., and D'esposito, M. (1998). The variability of human BOLD hemodynamic responses. *Neuroimage*. 8 (4), 360-369.
10. Mather, George. "The Visual Cortex". School of Life Sciences: University of Sussex.
University of Sussex.
11. DeAngelis, G. C.; Ohzawa, I.; Freeman, R. D. (1995). "Receptive field dynamics in the central visual pathways". *Trends in Neurosciences*. 18 (10): 451–457.
12. Yacoub, E. et al. (2003), Spin-echo fMRI in humans using high spatial resolutions and high magnetic fields. *Magn. Reson. Med.*, 49: 655-664.
13. Frank Tong, Ken Nakayama, Morris Moscovitch, Oren Weinrib & Nancy, Kanwisher (2000) Response Properties of the Human Fusiform Face Area. *Cognitive Neuropsychology*, 17:1-3, 257-280.
14. Duchaine, B., & Yovel, G. (2015). A Revised Neural Framework for Face Processing. *Annual Review of Vision Science*, 1(1), 393–416.
15. Wandell, B. A., & Winawer, J. (2015). Computational neuroimaging and population receptive fields. *Trends in Cognitive Sciences*, 19(6), 349–357.